A Nanoparticle Catalyst for Heterogeneous Phase Para-Hydrogen-Induced Polarization in Water

ARTICLE *in* ANGEWANDTE CHEMIE · JANUARY 2015

DOI: 10.1002/ange.201409027

7 AUTHORS, INCLUDING:

Yavuz Nuri Ertas
University of California, Los Angeles
8 PUBLICATIONS **29** CITATIONS
SEE PROFILE

Shawn Wagner
Cedars-Sinai Medical Center
47 PUBLICATIONS **880** CITATIONS
SEE PROFILE

Nuclear-Spin Polarization

DOI: 10.1002/anie.201409027

A Nanoparticle Catalyst for Heterogeneous Phase Para-Hydrogen-Induced Polarization in Water**

*Stefan Glöggler, Alexander M. Grunfeld, Yavuz N. Ertas, Jeffrey McCormick, Shawn Wagner, P. Philipp M. Schleker, and Louis-S. Bouchard**

Abstract: *Para-hydrogen-induced polarization (PHIP) is a technique capable of producing spin polarization at a magnitude far greater than state-of-the-art magnets. A significant application of PHIP is to generate contrast agents for biomedical imaging. Clinically viable and effective contrast agents not only require high levels of polarization but heterogeneous catalysts that can be used in water to eliminate the toxicity impact. Herein, we demonstrate the use of Pt nanoparticles capped with glutathione to induce heterogeneous PHIP in water. The ligand-inhibited surface diffusion on the nanoparticles resulted in a ^{1}H polarization of $P = 0.25\,\%$ for hydroxyethyl propionate, a known contrast agent for magnetic resonance angiography. Transferring the ^{1}H polarization to a ^{13}C nucleus using a para-hydrogen polarizer yielded a polarization of 0.013 %. The nuclear-spin polarizations achieved in these experiments are the first reported to date involving heterogeneous reactions in water.*

Nuclear magnetic resonance (NMR) is a powerful analytical technique that is widely used in chemistry and biomedicine. However, it exhibits sensitivity problems limiting its applications. Hyperpolarization techniques are designed to amplify detectable magnetization from nuclear spins by four orders of magnitude relative to thermal polarizations. These substantial signal enhancements facilitate detection of molecules in low concentrations. Hyperpolarization implicates a wide range of applications, from structural biology[1–3] to quantum computation,[4] operando investigations of catalytic reactors,[5,6] molecular imaging, and in vivo diagnostics.[7–13] The para-hydrogen-induced polarization (PHIP) method utilizes the singlet spin order of para-hydrogen to create hyperpolarization by incorporating hydrogen from para-hydrogen into a molecule of interest, or by a catalyst-mediated, reversible exchange process.[14–17]

PHIP has primarily been used in the investigation of chemical structures,[18] in gas–solid reactors,[5,6] and in the detection of cancer.[9,10] In vivo applications have encountered difficulties: a) heterogeneous catalysts employ organic solvents, none of which are biocompatible,[30,31] and b) rhodium complexes as homogeneous catalysts bear a risk of toxicity.[19,20] We focus on heterogeneous catalysts which have the advantage of easier separation from the substrate of interest, thereby mitigating toxicity issues. To overcome the challenges, we introduced a heterogeneous phase catalyst dispersed in water yielding hyperpolarization. Our catalyst construct consists of platinum nanoparticles capped with glutathione ligands.[21] The ligands cover a large fraction of the adsorption sites on the particles, leading to the detected polarization. For the hyperpolarization of 2-hydroxyethyl acrylate (HEA), which is considered the standard molecule for PHIP experiments in water and for in vivo angiography studies,[19,22–24] this nanoparticle design emerges as a heterogeneous alternative to existing prevalent homogeneous catalysts. This work opens the door to the production of biomedical imaging PHIP contrast agents free of catalysts.

Figure 1 summarizes the synthesis and characterization of the nanoparticles, which were synthesized from hexachloroplatinic acid and capped with glutathione[21] (Figure 1a; full details of the process can be found in the Supporting Information). Transmission electron microscopy (TEM) revealed that the nanoparticles have an average size of 2.0 nm (Figure 1b). The capping of the nanoparticles is

[*] Dr. S. Glöggler, A. M. Grunfeld, M. Sc. J. McCormick, Prof. L.-S. Bouchard
Department of Chemistry and Biochemistry
University of California at Los Angeles
607 Charles E Young Drive East, Los Angeles, CA 90095-1569 (USA)
E-mail: bouchard@chem.ucla.edu
M. Sc. Y. N. Ertas, Prof. L.-S. Bouchard
Department of Bioengineering
University of California at Los Angeles
607 Charles E Young Drive East, Los Angeles, CA 90095-1569 (USA)
Prof. S. Wagner
Biomedical Imaging Research Institute
Cedars Sinai Medical Center, 8700 Beverly Blvd
Davis Building G149E, Los Angeles, CA 90048 (USA)
Dipl.-Chem. P. P. M. Schleker
Institute für Technische and Makromolekulare Chemie
RWTH Aachen University
Worringer Weg 1, 52074 Aachen (Germany)
Prof. L.-S. Bouchard
California NanoSystems Institute
University of California at Los Angeles, 570 Westwood Plaza
Building 114, Los Angeles, CA 90095-1569 (USA)

[**] The authors gratefully acknowledge financial support from the NSF, grant CHE-1153159, equipment grant CHE-1048804, the Arnold and Mabel Beckman Foundation, the Jonsson Comprehensive Cancer Center Foundation at UCLA and support by the German Academic Exchange Service (DAAD) through its Thematic Network "ACalNet" funded by the German Federal Ministry of Education and Research (BMBF).

Supporting information for this article is available on the WWW under http://dx.doi.org/10.1002/anie.201409027.

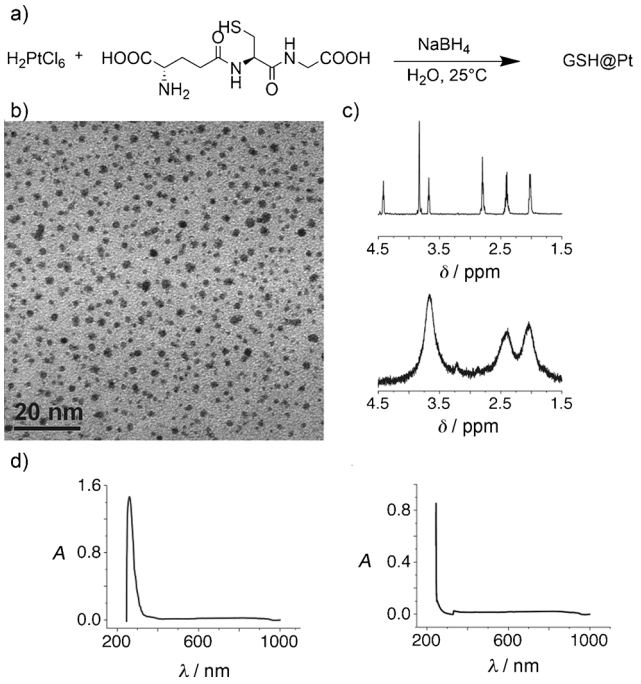

Figure 1. Synthesis and characterization of the nanoparticles. a) Glutathione (GSH) and H_2PtCl_6 in water are reduced with $NaBH_4$ to yield GSH-capped Pt nanoparticles. b) TEM image of the nanoparticles, showing an average size of 2.0 ± 0.6 nm. c) ^{1}H NMR spectra of GSH in D_2O (top) and of GSH capped onto the surface of the Pt nanoparticles (bottom). The line broadening indicates that ligands have bound to the surface. Both spectra were acquired at $B_0 = 14.1$ T (600 MHz proton frequency). d) UV/Vis absorption spectra of H_2PtCl_6 in water (left) and of the suspended nanoparticles (right).

confirmed by ^{1}H NMR spectroscopy using the following experiment. When glutathione is dissolved in solution, narrow resonance signals attributable to the functional groups in the molecule are detected (Figure 1c, top spectrum). During capping of the nanoparticles, interactions between the ligands and the surfaces of the particles cause a broadening of these signals as a result of dipolar interactions, indicating that the capping procedure is successful (Figure 1c). The capping was additionally confirmed by thermogravimetric analysis (see the Supporting Information).

Subsequently, we investigated a potential problem that might arise during the reduction and cleaning of the particles, that is, residual hexachloroplatinic acid, a soluble metal complex in water, could act as the catalytic center instead of the nanoparticles. To ensure the desired exclusive presence of platinum particles, UV/Vis absorption spectra of both the reactant and the nanoparticles were recorded (Figure 1d). With platinum ions present, an absorption peak at $\lambda = 260$ nm was recorded. Although this peak was detected for hexachloroplatinic acid, it did not occur with nanoparticles dispersed in water, implying that the platinum particles were responsible for catalyzing the hydrogenation reaction.

Additionally, a mercury-poisoning test was performed to confirm that the hydrogenation occurs due to the platinum particles and not due to platinum ions. The reaction of HEA with hydrogen was initiated and upon addition of mercury, no further conversion into the propionate was detected.[26]

Possible leaching of surface ligands attached to the nanoparticles did not appear during the hydrogenation experiments, as confirmed by a noticeable dipolar broadening of resonance signals in the resultant ^{1}H NMR spectrum. Even if the ligands were to leach, glutathione would be biocompatible within the human body, acting as an antioxidant.[25]

To achieve hyperpolarization by PHIP, a pairwise addition of para-hydrogen to a molecule of interest is required.[27] The pairwise addition of a para-hydrogen molecule implies that its nuclear-spin singlet state is preserved during the hydrogenation process. Without this preservation, signal enhancement would not be possible. A hyperpolarized signal becomes detectable if the incorporation of para-hydrogen has occurred at two magnetically nonequivalent sites. Previous studies[28–31] demonstrated that nanoparticles enabled the preservation of the required quantum correlation in other contexts, with the greatest success achieved for reactions in the gas phase.[6] PHIP with nanoparticles in the liquid phase was previously reported, but the reaction was performed in non-biocompatible solvents, preventing in vivo applications.[30,31] Sufficiently small ligand-capped nanoparticles lead to hyperpolarization because of the restriction of the hydrogen diffusion on the nanoparticle surface which inherently results in more pairwise additions (Figure 2b).[29] Larger and uncapped particles result

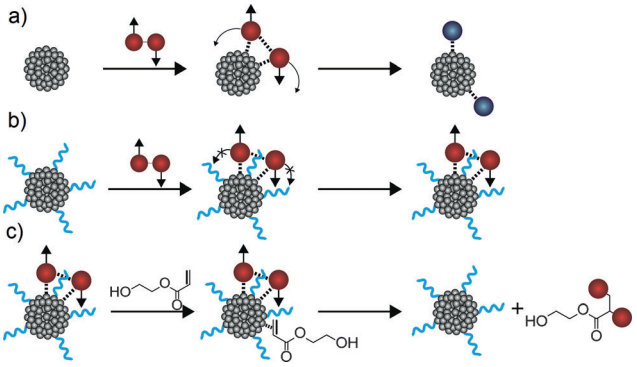

Figure 2. a) Para-hydrogen (red circles represent hydrogen with quantum correlation) that adsorbs onto the surface of bare Pt nanoparticles (gray circles) is prone to randomization processes leading to the loss of quantum correlation (blue circles). b) If ligands are attached to the surface of the nanoparticles (blue lines), the randomization can be partly avoided, resulting in preservation of the singlet state between the two protons. c) As a result of the preserved singlet state on the surface of the glutathione-capped nanoparticles, para-hydrogen can be used to generate hyperpolarized products in water.

in randomization of the nuclear spin correlations without hyperpolarization (Figure 2a).[28,29] Glutathione nanoparticles can be easily dispersed in water, enabling the hydrogenation of HEA to 2-hydroxyethyl propionate. This is schematically presented in Figure 2c.

The hydrogenated species show two distinct hyperpolarized signals around $\delta = 1.1$ ppm and 2.5 ppm in the ^{1}H NMR spectrum (Figure 3). Figure 3a shows the hyperpolarized spectrum of 2-hydroxyethyl propionate acquired in a magnetic field of $B_0 = 14.1$ T (600 MHz proton frequency) yielding a polarization of $P = 0.25\,\%$, a 50-fold signal enhancement

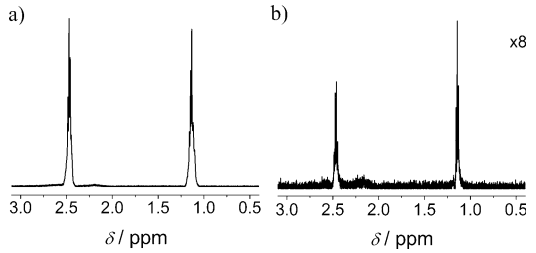

Figure 3. a) ^{1}H NMR spectrum of the hyperpolarized region of 2-hydroxyethyl propionate. A polarization of $P = 0.25\,\%$ was achieved. The spectrum is shown in absolute values. b) Thermally polarized spectrum of the same region for comparison. The spectrum was magnified by a factor of 8.

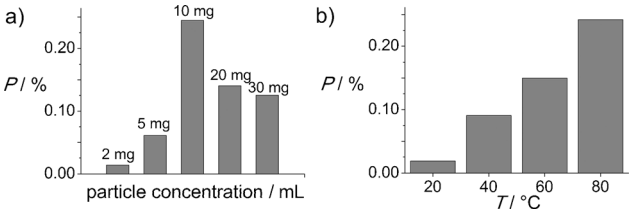

Figure 4. a) Histogram showing polarization (P) as a function of particle concentration. The maximum polarization for Pt-capped nanoparticles was achieved for a concentration of 10 mg mL^{-1}. b) Polarization values plotted as a function of temperature, with increased polarization observed with increasing temperature. At 80 °C a polarization of $P = 0.25\,\%$ was achieved following a 10 s transport process before detection.

compared to the signal achieved from thermal equilibrium at 14.1 T. To calibrate the signal, a spectrum was acquired at thermal equilibrium after hydrogenation with the same sample (Figure 3b). The proton longitudinal relaxation time of the hyperpolarized protons was measured to be 3 s at 14.1 T. In a typical PHIP experiment, the sample is pressurized with para-hydrogen, followed by sample mixing. In our experiments, the subsequent transport of the polarized substrate to the magnet took 10 s, resulting in an up to tenfold loss in the polarization following the chemical reaction. Higher polarizations should be attainable by shortening the travel time. We attribute the observation of the effect mainly to the nature of the applied ligands. To verify our assumption, a different experiment with mercaptobenzoic acid capped nanoparticles was conducted.[29] These particles were also dispersible in water but were slightly larger (2.5 nm instead of 2.0 nm).[29] However, no para-hydrogen-derived signal could be generated.

The crucial differentiator between previously used particles and the glutathione-capped particles is the extent of the ligand coverage of the surface of the glutathione-capped particles, which is higher by almost a factor of two (23 wt % instead of 13 wt %[29]). Per molecule, up to two binding sites of the glutathione ligand (amine and thiol moieties) can coordinate to the particles' surface.[32] As a result, more sites for adsorption of para-hydrogen are blocked with increasing ligand coverage and diffusion on the surface is partly obstructed, hampering the randomization process of the para spin state.

We explored the dependence of polarization on particle concentration and sample temperature (Figure 4a). When the particle concentration was varied, increases in polarization were measured. At lower concentrations (< 10 mg mL^{-1}), the pairwise addition of para-hydrogen proceeds too slowly because there is not enough catalyst, thereby decreasing polarization yields. On the other hand, when the particle concentration is too high, the particles grow less dispersed and agglomerate. In this case, the randomization processes become more prominent and the singlet state is lost. The reaction rate can also be controlled by changing the temperature (Figure 4b). In temperature variation experiments (particle concentration = 10 mg mL^{-1}), a polarization of $P = 0.02\,\%$ was observed at 20 °C, which is only four times larger than the polarization achievable in thermal equilibrium in a magnetic field of $B_0 = 14.1$ T. As the temperature was increased, the obtained hyperpolarization increased accordingly, up to a maximum polarization of 0.25 % at 80 °C. The given temperatures represent the initial state. Upon pressurization of the NMR tube with hydrogen, the sample temperature decreased and continued to do so during the mixing procedure (see the Supporting Information for experimental details). Consequently, the measured polarization values were effectively generated at temperatures lower than those initially measured.

We evaluated our heterogeneous catalyst against the standard PHIP homogeneous catalyst, 1,4-bis-[(phenyl-3-propane sulfonate) phosphine]butane rhodium(I) tetrafluoroborate.[19] Experiments with the homogeneous catalyst exhibited a polarization of $P = 1.26\,\%$ at 80 °C. Furthermore, the polarization yields with the homogeneous catalysts are less affected by temperature: at 20 °C, the polarization showed $P = 0.7\,\%$. Despite gaining higher polarization with the homogeneous catalyst, the nanoparticles reveal an important benefit; they can be separated from the reaction solution by centrifugation or by evaporation of the solvent after use and thus can be reused for additional hyperpolarization experiments (see the Supporting Information).[33] In recycling experiments, the nanoparticles were reused five times without showing any loss in activity or decrease in signal enhancement. Additionally, use of the supernatant solvent did not give rise to catalytic activity, providing further evidence that the hyperpolarization is generated by nanoparticles.

Ultimately, proton polarization may not be the most useful form for in vivo applications because of the short ^{1}H spin–lattice relaxation time (typically 1–3 seconds). ^{13}C polarization is of greater interest because of its longer relaxation times in biologically relevant molecules, which can sometimes exceed one minute.[20] ^{13}C polarization is normally obtained in a PHIP experiment using polarizer equipment. Automated hyperpolarization devices that apply polarization-transfer sequences and operate with a homogeneous catalyst heated to 60 °C are capable of generating over 10 % ^{13}C polarization.[23] We utilized a similar device to transfer the polarization of hyperpolarized protons in hydroxyethyl propionate (^{13}C- and ^{2}H-enriched) to its carbonyl carbon, with the hydrogenation reaction catalyzed by the nanoparticles (Figure 5).[34] The achieved polarization ($P = 0.013\,\%$) was

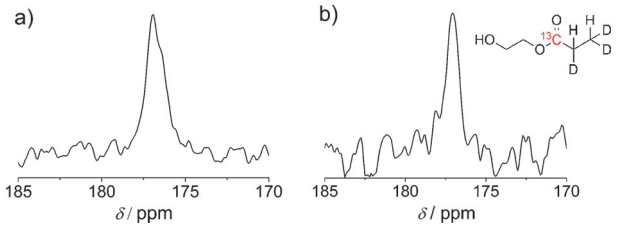

Figure 5. a) ^{13}C NMR signal of hyperpolarized hydroxyethyl propionate at $B_0 = 9.4$ T and b) thermally polarized hydroxyethyl propionate recorded with 16 scans. In both cases, a line broadening of 20 Hz was applied.

16 times larger, compared to a sample in thermal equilibrium at 9.4 T, following a transit time to the magnet of 20 s. We deduct from this result that such experiments may require a redesign of current para-hydrogen polarizers for use with heterogeneous catalysts that allow for a better mixing at stable temperatures and improved polarization-transfer sequences (see the Supporting Information).

The current setup would achieve $P = 10\,\%$ ^{13}C polarization with a homogeneous catalyst, whereas the proton polarization measurements in our study with the heterogeneous catalyst resulted in five times less polarization. On this basis, we project that with optimized equipment a ^{13}C polarization in the magnet of at least 2% is feasible, which would be sufficient for in vivo imaging.[35]

This demonstration of the first heterogeneous phase PHIP in water by utilizing glutathione-capped Pt nanoparticles yielded a substantial polarization in water with a heterogeneous catalyst. 2-hydroxyethyl propionate was hyperpolarized in water to a significant extent using the presented heterogeneous catalyst. The key features and main advances of this system are the biocompatibility of glutathione-capped ligands, the dispersibility of the catalyst in water, the potential for immobilizing the nanoparticles in a reactor or filtering them, and the recyclability of the nanoparticles. We further found that particle concentration and temperature are critical to the generation of strongly hyperpolarized substrates in solution, suggesting that precise refinement is necessary for process optimization. We expect the successful development of an effective yet removable heterogeneous catalyst to play a pivotal role in the expansion of biomedical molecular-imaging applications for the detection of cancer and other conditions.[10]

Received: September 12, 2014
Revised: November 18, 2014
Published online: ■■ ■■, ■■■■

Keywords: heterogeneous catalysis · hyperpolarization · nanoparticles · NMR spectroscopy · para-hydrogen

[1] I. Gelis, V. Vitzthum, N. Dhimole, M. A. Caporini, A. Schedlbauer, D. Carnevale, S. R. Connell, P. Fucini, G. Bodenhausen, *J. Biomol. NMR* **2013**, *56*, 85 – 93.
[2] A. H. Linden, S. Lange, W. T. Franks, U. Akbey, E. Specker, B.-J. Van Rossum, H. Oschkinat, *J. Am. Chem. Soc.* **2011**, *133*, 19266 – 19269.
[3] M. Rosay, A.-C. Zeri, N. S. Astrof, S. J. Opella, J. Herzfeld, R. G. Griffin, *J. Am. Chem. Soc.* **2001**, *123*, 1010 – 1011.
[4] S. Simmons, R. M. Brown, H. Riemann, N. V. Abrosimov, P. Becker, H.-J. Pohl, M. L. W. Thewalt, K. M. Itoh, J. J. L. Morton, *Nature* **2011**, *470*, 69 – 72.
[5] L.-S. Bouchard, S. R. Burt, M. S. Anwar, K. V. Kovtunov, I. V. Koptyug, A. Pines, *Science* **2008**, *319*, 442 – 445.
[6] N. N. J. Jarenwattananon, S. Glöggler, T. Otto, A. Melkonian, W. Morris, S. R. Burt, O. M. Yaghi, L.-S. Bouchard, *Nature* **2013**, *502*, 537 – 540.
[7] K. Golman, R. in't Zandt, M. Lerche, R. Pehrson, J. H. Ardenkjaer-Larsen, *Cancer Res.* **2006**, *66*, 10855 – 10860.
[8] S. E. Day, M. I. Kettunen, F. A. Gallagher, D.-E. Hu, M. Lerche, J. Wolber, K. Golman, J. H. Ardenkjaer-Larsen, K. M. Brindle, *Nat. Med.* **2007**, *13*, 1382 – 1387.
[9] K. Golman, O. Axelsson, H. Johannesson, S. Mansson, C. Olofsson, J. S. Petersson, *Magn. Reson. Med.* **2001**, *46*, 1 – 5.
[10] P. Bhattacharya, E. Y. Chekmenev, W. H. Perman, K. C. Harris, A. P. Lin, V. A. Norton, C. T. Tan, B. D. Ross, D. P. Weitekamp, *J. Magn. Reson.* **2007**, *186*, 150 – 155.
[11] J. P. Muggler III, B. Driehuys, J. R. Brookeman, G. D. Cates, S. S. Berr, R. G. Bryant, T. M. Daniel, E. E. De Lange, J. H. Downs, C. J. Erickson, W. Happer, D. P. Hinton, N. F. Kassel, T. Maier, C. D. Phillips, B. T. Saam, K. L. Sauer, M. E. Wagshul, *Magn. Reson. Med.* **1997**, *37*, 809 – 815.
[12] J. P. Muggler III, T. A. Altes, I. C. Ruset, I. M. Dregely, J. F. Mata, G. W. Miller, S. Ketel, J. Ketel, F. W. Hersman, K. Ruppert, *Proc. Natl. Acad. Sci. USA* **2010**, *107*, 21707 – 21712.
[13] D. A. Lipson, D. A. Roberts, J. Hansen-Flaschen, T. R. Gentile, G. Jones, A. Thompson, I. E. Dimitrov, H. I. Palevsky, J. S. Leigh, M. Schnall, R. R. Rizi, *Magn. Reson. Med.* **2002**, *47*, 1073 – 1076.
[14] C. R. Bowers, D. P. Weitekamp, *Phys. Rev. Lett.* **1986**, *57*, 2645 – 2648.
[15] C. R. Bowers, D. P. Weitekamp, *J. Am. Chem. Soc.* **1987**, *109*, 5541 – 5542.
[16] T. C. Eisenschmid, R. U. Kirss, P. P. Deutsch, S. I. Hommeltoft, R. Eisenberg, J. Bargon, R. G. Lawler, A. L. Balch, *J. Am. Chem. Soc.* **1987**, *109*, 8089 – 8091.
[17] R. W. Adams, J. A. Aguilar, K. D. Atkinson, M. J. Cowley, P. I. P. Elliott, S. B. Duckett, G. G. R. Green, I. G. Khazal, J. Lopez-Serrano, D. C. Williamson, *Science* **2009**, *323*, 1708 – 1711.
[18] S. B. Duckett, C. J. Sleigh, *Prog. Nucl. Magn. Reson. Spectrosc.* **1999**, *34*, 71 – 92.
[19] K. W. Waddell, A. M. Coffey, E. Y. Chekmenev, *J. Am. Chem. Soc.* **2011**, *133*, 97 – 101.
[20] R. V. Shchepin, A. M. Coffey, K. W. Waddell, E. Y. Chekmenev, *J. Phys. Chem. Lett.* **2012**, *3*, 3281 – 3285.
[21] S. E. Eklund, D. E. Cliffel, *Langmuir* **2004**, *20*, 6012 – 6018.
[22] M. Goldman, H. Johannesson, O. Axelsson, M. Karlsson, *Magn. Reson. Imaging* **2005**, *23*, 153 – 157.
[23] M. Goldman, H. Johannesson, O. Axelsson, M. Karlsson, *C. R. Chim.* **2006**, *9*, 357 – 363.
[24] M. Roth, P. Kindervater, H.-P. Raich, J. Bargon, H. W. Spiess, K. Münnemann, *Angew. Chem. Int. Ed.* **2010**, *49*, 8358 – 8362; *Angew. Chem.* **2010**, *122*, 8536 – 8540.
[25] J. D. Hayes, L. I. McLellan, *Free Radical Res.* **1999**, *31*, 273 – 300.
[26] R. H. Crabtree, *Chem. Rev.* **2012**, *112*, 1536 – 1554.
[27] R. A. Green, R. W. Adams, S. B. Duckett, R. E. Mewis, D. C. Williamson, G. G. R. Green, *Prog. Nucl. Magn. Reson. Spectrosc.* **2012**, *67*, 1 – 48.
[28] K. V. Kovtunov, I. E. Beck, V. I. Bukhtiyarov, I. V. Koptyug, *Angew. Chem. Int. Ed.* **2008**, *47*, 1492 – 1495; *Angew. Chem.* **2008**, *120*, 1514 – 1517.
[29] R. Sharma, L.-S. Bouchard, *Sci. Rep.* **2012**, *2*, 277.
[30] A. M. Balu, S. B. Duckett, R. Luque, *Dalton Trans.* **2009**, 5074 – 5076.

[31] M. Irfan, N. Eshuis, P. Spannring, M. Tessari, M. C. Feiters, F. P. J. T. Rutjes, *J. Phys. Chem. C* **2014**, *118*, 13313 – 13319.
[32] A. A. Sousa, J. T. Morgan, P. H. Brown, A. Adams, M. P. SureshJayasekara, G. Zhang, C. J. Ackerson, M. J. Kruhlak, R. D. Leapman, *Small* **2012**, *8*, 2277 – 2286.
[33] D. Astruc, F. Lu, J. R. Aranzaes, *Angew. Chem. Int. Ed.* **2005**, *44*, 7852 – 7872; *Angew. Chem.* **2005**, *117*, 8062 – 8083.
[34] J. Agraz, A. Grunfeld, K. Cunningham, D. Li, S. Wagner, *J. Magn. Reson.* **2013**, *235*, 77 – 84.
[35] S. J. Kohler, Y. Yen, J. Wolber, A. P. Chen, M. J. Albers, R. Bok, V. Zhang, J. Tropp, S. Nelson, D. B. Vigneron, J. Kurhanewicz, R. E. Hurd, *Magn. Reson. Med.* **2007**, *58*, 65 – 69.

Communications

Nuclear-Spin Polarization

S. Glöggler, A. M. Grunfeld, Y. N. Ertas, J. McCormick, S. Wagner, P. P. M. Schleker, L.-S. Bouchard* _____ ■■■–■■■

A Nanoparticle Catalyst for Heterogeneous Phase Para-Hydrogen-Induced Polarization in Water

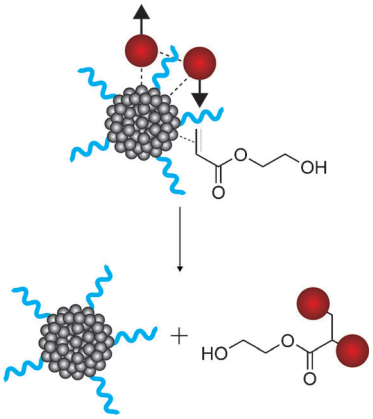

Hyperpolarization of molecules utilizing para-hydrogen (red spheres; see picture) and Pt nanoparticles (gray spheres) in water is described. The nanoparticles (diameter ≈ 2 nm) are capped with glutathione ligands (blue lines) to allow for the pairwise addition of para-hydrogen and create observable magnetization. As the solvent is biocompatible, the generation of new molecular imaging contrast agents can be envisioned.